Aquat. Living Resour. 2019, 32, 18

https://doi.org/10.1051/alr/2019015

Aquatic Living Resources
Available online at:
www.alr-journal.org

Research Article

Population genetics and molecular phylogeography of *Thamnaconus modestus* (Tetraodontiformes, Monachanthidae) in Northwestern Pacific inferred from variation of the mtDNA control region

Tianyan Yang[1], Zhiyang Wang[2], Yong Liu[3], and Tianxiang Gao[1,*]

[1] Fisheries College, Zhejiang Ocean University, Zhoushan, PR China
[2] School of Ocean, Yantai University, Yantai, PR China
[3] Key Laboratory of South China Sea Fishery Resources Exploitation & Utilization, Ministry of Agriculture, P.R. China, Guangzhou, PR China

Received 2 April 2019 / Accepted 16 June 2019

Handling Editor: Carlos Saavedra

Abstract – In order to study the genetic diversity of *Thamnaconus modestus*, a species of great commercial importance in Southeast Asia, the 5′-end hypervariable regions (423 bp) of the mitochondrial control region of *T. modestus* in nine geographical populations (248 individuals) were sequenced and analysed in this study. The target sequence fragment contained large numbers of polymorphic sites (87) involved in high levels of haplotype diversity ($h = 0.97 \pm 0.01$) and nucleotide diversity ($\pi = 0.0285 \pm 0.0143$). The genetic variations within populations (92.71%) were significantly larger than those among populations (7.29%). No significant genetic divergences were detected among the wild populations owing to their gregarious habits, strong moving ability, r-selection strategy. Significant genetic divergences were found between the cultured and wild populations, probably resulting from kin selection and aquacultural environment. Three significant phylogenetic lineages were identified, and the variation among lineages (56.90%) was greater than that among individuals within the lineages (43.10%), with the significant Φ_{ST} value ($\Phi_{ST} = 0.57$, $P = 0.0000$). The results showed great and significant genetic differentiations among these three lineages, indicating that they may have independent phylogenetic dynamics. Dominant shared haplotypes that included individuals from each population and the median-joining network of haplotypes presented a star-like structure. Historic demographic analysis of each lineage showed that population expansion occurred after the Pleistocene glacial period. At the last glacial maximum, *T. modestus* in China seas was scattered across variable refuges, including Central South China Sea and Okinawa Trough.

Keywords: *Thamnaconus modestus* / mitochondrial DNA / population genetic structure / phylogenetics / demographic analysis

1 Introduction

The black scraper *Thamnaconus modestus* is a warm-water benthic fish (7–120-m depth) with a wide geographic distribution in Indo-Northwest Pacific Ocean, from Hokkaido in the north to Northern South China Sea in the south (Su and Li, 2002). It has obvious migratory habits with long-distance migration and stable route characteristics (Yamada et al., 2007).

China has a history of over ten years in utilizing *T. modestus* resources. Given the abundant fishery resources and the convenience of fishing, it has become an important economic fishing target (maximum annual output of 340,000 tons in 1987) in China next to *Trichiurus lepturus* by the end of the 1980s (Qian and Hu, 1980; Zheng et al., 1990). However, due to overfishing and environmental changes, such as marine pollution, devastation on marine ecology and climatic change, the *T. modestus* yield in China has been sharply declining to 2000 tons in 1995 (Chen et al., 2000). In Korea, total catches of 230,000 tons were harvested annually until 1990, since then the landings have been declined continuously, and the lowest

*Corresponding author: gaotianxiang0611@163.com

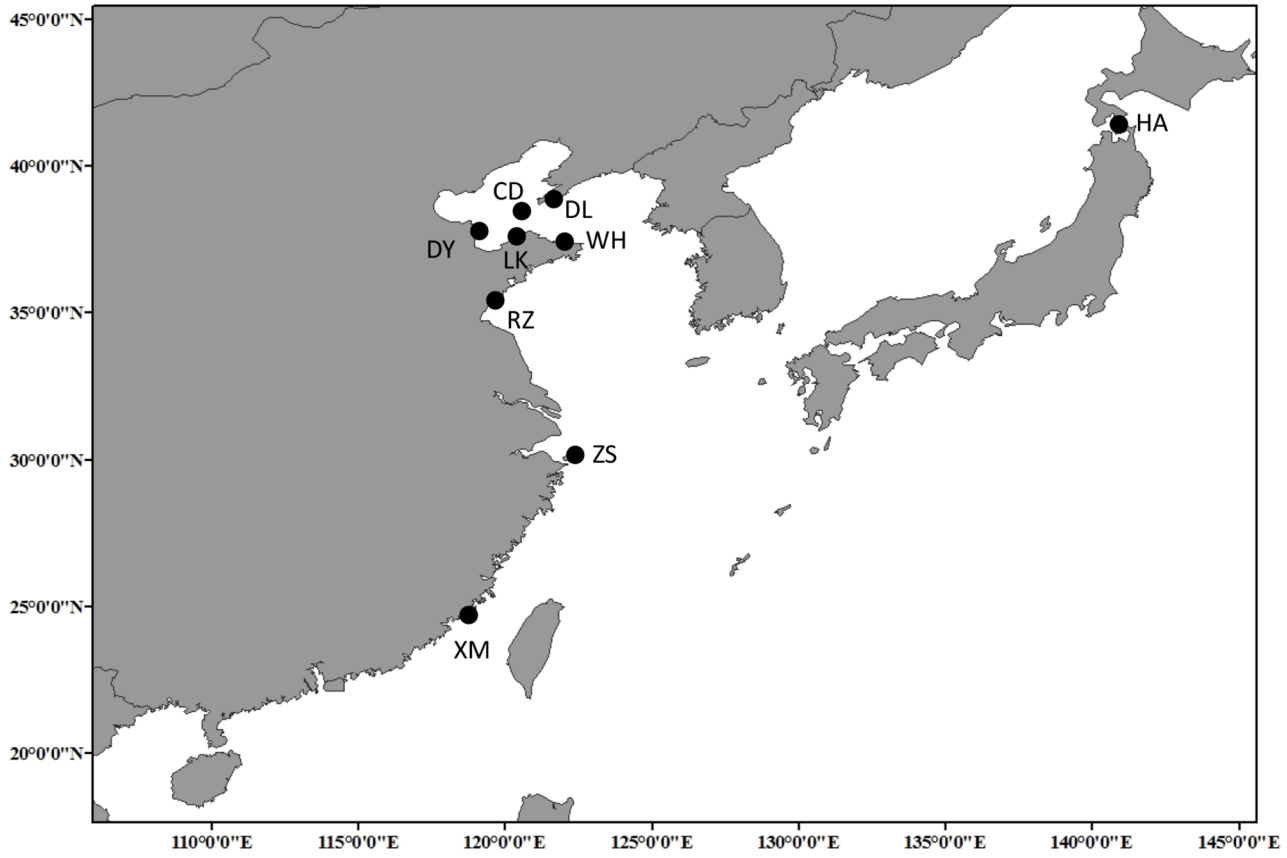

Fig. 1. Map of the sample locations of *T. modestus*.

documented catch was only 933 tons in 2002 (NFRDI, 2009). Meanwhile, the catch in Japan has always been low according to the statistics data of United Nations Food and Agriculture Organization (FAO) over the past 20 years.

Previous fishery biology studies on population composition, distribution characters and geographically classification have demonstrated that the *T. modestus* that inhabits East Yellow Sea and Southwestern Japan Sea could be divided into two major local populations in terms of the multivariate statistical analysis of morphological characteristics, reproductive spatial isolation and population dynamics regularity (Wang, 1988; Zheng et al., 1990). One is the Japanese Sea local population and the other is the East China Sea and Yellow Sea-Korean Peninsula local population. The latter is further divided into four groups, i.e. the Northern Yellow Sea group, the Coastal Korean Peninsula group, the offshore group of East China Sea and the Southern East China Sea group (Zheng et al., 1990). Different groups have unique ecological habits (e.g. feeding ground location and spawning time) and external morphological variations because of different natural environmental conditions and hereditary factors.

The existing research works on *T. modestus* have mostly concentrated on population identification, resource assessment and biology fields (Kwon et al., 2007; Mizuno et al., 2012; An et al., 2013; Kim et al., 2016; Hatab et al., 2017; Miyajima-Taga et al., 2017), but the population distribution pattern of *T. modestus* in Northwestern Pacific from the molecular genetics perspective remains unclear. The artificial propagation of *T. modestus* has made a significant breakthrough in China in recent years (Li et al., 2002; Liu et al., 2017). Therefore, investigating genetic diversity and clarifying genetic background are of great significance in black scraper aquaculture for selective breeding in the future. In this study, we discussed the molecular phylogeny of *T. modestus*, clarified its population genetic diversity and speculated on the demographic history based on mitochondrial DNA control region sequences. Our results provide helpful suggestions for resource management and the sustainable utilisation of *T. modestus* in the future.

2 Materials and methods

2.1 Sample collection

From October 2010 to January 2016, 248 *T. modestus* specimens were collected from nine locations (Hakodate-HA $n = 22$, Dalian-DL $n = 32$, Dongying-DY $n = 19$, Longkou-LK $n = 50$, Changdao-CD $n = 25$, Weihai-WH $n = 27$, Rizhao-RZ $n = 32$, Zhoushan-ZS $n = 30$, Xiamen-XM $n = 30$) distributed from north of Japan Sea to south of East Hainan Province (Fig. 1), among which the specimen from Longkou (LK) was a cultured population, while the others were wild populations. The muscle tissues were soaked with absolute ethanol and preserved at −20 °C refrigeration.

2.2 Genomic DNA extraction and PCR amplification

The muscle tissues were digested in 500 μL of DNA lysis buffer [0.1 mol/L of NaCl, 10 mmol/L of Tris–Cl (pH 8.0), 1 mmol/L of EDTA (pH 8.0)] and 25 μL of 20% (W/V) sodium dodecyl sulphate (SDS) containing 15 μL of Proteinase K (20 mg/mL, Merck). The mixture solution was placed in a 50 °C thermostat water bath for 2 h. The total genomic DNA was isolated using the standard phenol/chloroform extraction method (Sambrook and Russell, 2001).

Forward primer DL-S (5′-CCCACCACTAACTCC-CAAAGC-3′) and reverse primer DL-R (5′-CTGGAAA-GAACGCCCGGCATG-3′) were used to amplify the segment sequence of the mtDNA control region (Liu et al., 2010; Song et al., 2013). The PCR reaction was performed in a volume of 25 μL containing 25 ng template DNA, 2.5 μL of 10× reaction buffer, 2 μL of dNTPs (10 mM), 0.5 μL each of primer (20 μM) and 1 U Taq DNA polymerase (TaKaRa, Japan). The parameters of PCR amplifications consisted of the initial denaturation at 94 °C for 5 min followed by 35 cycles at 94 °C for 30 s, 52 °C for 30 s and 72 °C for 45 s and a final extension at 72 °C for 10 min and then held at 4 °C. Amplification products were detected by 1.0% agarose gel electrophoresis. Meanwhile, negative controls (template-free PCR reactions) were prepared to ensure the fidelity of the PCR reactions. The PCR products were purified using a QIAquick PCR Purification Kit (Qiagen, Germany) and direct-bidirectionally sequenced by BigDye® Terminator Ready Reaction mix (Applied Biosystems) with an ABI Prism 3700 automated DNA sequencer.

2.3 Sequence analysis

The control region sequences were proofread, aligned and edited by the DNAStar software package under the default parameters scenario. The best-fitting nucleotide substitution model, TrN+G, was subjected to the hierarchical likelihood ratio test implemented in the jModelTest software (Darriba et al., 2012). DNASP version 6.1 (Rozas et al., 2017) and Arlequin 3.5 (Excoffier and Lischer, 2010) were used to detect the genetic differentiation and calculate the nucleotide polymorphism indexes, such as the haplotype diversity, the nucleotide diversity, the average pairwise nucleotide difference and the numbers of transition and transversion.

2.4 Population genetic structure analysis

The genetic variation between populations evaluated by the corrected average pairwise differences, the average number of pairwise differences and the pairwise fixation index (Φ_{ST}) was calculated in Arlequin 3.5 (Excoffier and Lischer, 2010) in which the significance of Φ_{ST} was determined by 10,000 permutations, and the *p*-value was corrected for multiple tests by the Bonferroni method (Rice, 1989). The same software was utilised for the analysis of molecular variance (AMOVA) to investigate the mutational differences among different populations, with the significance assessed by 10,000 permutations. The population's genetic structure was determined by the clustering algorithm implemented in the Bayesian Analysis of Population Structure 6.0 (BAPS) software (Corander et al., 2004). Calculations were performed with the initially fixed *k* (the number of clusters) varying from 2 to 30. Stochastic optimisation was used to infer the posterior model of the genetic structure. The highest natural logarithm of marginal likelihood of all haplotypes was selected to obtain the optimal population structure based on the genetic linkage model.

Network 5.0 was used to construct a haplotype network based on the median-joining method to directly reflect the relationship between haplotypes. *T. hypargyreus* was used as an outgroup. MrBayes (Ronquist et al., 2012) and IQ-TREE (Nguyen et al., 2015) were used to construct Bayesian inference (BI) and maximum likelihood (ML) trees, respectively. ML phylogenetic analysis was performed via IQ-TREE with 1000 bootstrap replicates, using default settings. BI analysis was run by MrBayes for 100,000 generations until the average standard deviation of split frequencies was lower than 0.01 in all cases. Topologies were sampled every 1000 generations, with the first 25% of the trees discarded as burn-in. The Markov chain Monte Carlo (MCMC) method was used to estimate the posterior distribution of model parameters.

2.5 Demographic history analysis

To evaluate whether the populations underwent rapid expansions, the R^2 statistical (Ramos-Onsins and Rozas, 2002; Domingues et al., 2018), Tajima'*D* (Tajima, 1989) and the Fu's *Fs* (Fu, 1997) tests (10,000 coalescent simulations) for deviation from neutrality were investigated using DNASP and Arlequin. Meanwhile, mismatch distribution analysis was also performed in Arlequin. The expected distribution under a model of sudden demographical expansion was generated using 10,000 permutations.

We used the Bayesian Evolutionary Analysis Sampling Trees (BEAST) 2.4.3 (Bouckaert et al., 2014) software package and Tracer 1.6 to create the Bayesian skyline plot (BSP) (Drummond and Bouckaert, 2015). Demographic analysis of all sequences was carried out with a piecewise-constant skyline model with 10 million generations (the first 1 million were discarded as burn-in). A strict molecular clock model was set, and the evolutionary rate was assumed to be 0.03–0.1/million years (Stewart and Baker, 1994; Iguchi et al., 1997; Donaldson and Wilson, 1999). MCMC analysis was performed four times independently for 10,000,000 generations each. After completing all runs, the Tracer software was utilised to examine the run convergence. Using this software, the Bayesian skyline could be constructed directly in the case of an effective sampling size (ESS) that is superior or equal to 200 for all parameters, suggesting the acceptable mixing and the sufficient sampling. Otherwise, the LOGCOMBINER program included in the BEAST software package was needed to discard the first 25% of the samples as burn-in and then combined with the two results to compare the analyses.

3 Results

3.1 Sequence characterisation and molecular diversity

A total of 87 variation sites were detected in 267 specimens, accounting for 20.57% of the total length of the

Table 1. Sample information and diversity index of *T. modestus*.

Population abbreviation	Sampling location	Sampling date	No. of individuals	No. of polymorphic sites	No. of haplotypes	No. of population-specific haplotypes	Haplotype diversity (h)	Nucleotide diversity (π)
HA	Hakodate	October, 2010	22	44	17	8	0.93 ± 0.05	0.0257 ± 0.0135
DL	Dalian	November, 2015	32	50	22	6	0.97 ± 0.02	0.0293 ± 0.0151
DY	Dongying	November, 2014	19	37	18	5	0.99 ± 0.02	0.0233 ± 0.0124
LK	Longkou	July, 2011	50	43	18	8	0.87 ± 0.03	0.0311 ± 0.0158
CD	Changdao	May, 2015	25	31	15	2	0.94 ± 0.03	0.0246 ± 0.0130
WH	Weihai	November, 2012	27	40	22	5	0.98 ± 0.02	0.0225 ± 0.0118
RZ	Rizhao	May, 2013	32	41	20	2	0.96 ± 0.02	0.0249 ± 0.0129
ZS	Zhoushan	January, 2016	30	50	22	5	0.97 ± 0.02	0.0285 ± 0.0148
XM	Xiamen	February, 2015	30	47	23	7	0.98 ± 0.02	0.0248 ± 0.0130
Total			267	87	82	48	0.97 ± 0.01	0.0285 ± 0.0143

sequence (423 bp) in which 65 parsimony informative, 5 insertion/deletion, 79 transformation and 5 transmutation sites were observed. Eighty-two haplotypes were defined, including 48 population-specific and 35 shared haplotypes (Tab. 1).

Among all wild populations, the haplotype diversity (h) was highest in DY (0.99 ± 0.02) and lowest in HA (0.93 ± 0.05). The haplotype diversity in the cultured population (LK) was the lowest of all (0.87 ± 0.03), but the nucleotide diversity (π) was the highest (0.0311 ± 0.0158). The overall haplotype diversity and the nucleotide diversity were 0.97 ± 0.01 and 0.0285 ± 0.0143, respectively.

3.2 Genetic structure

The results of the Bayesian cluster analysis (Fig. 2) suggested three lineages of all haplotypes, with the maximum value of the marginal likelihood logarithm was −1433.6052. According to the results of Bayesian clustering and the topological structure of phylogenetic trees, all haplotypes were divided into three lineages (Fig. 3). The haplotype of each population presented scattered distribution, and the pedigree structure did not correspond to the geographical distribution. The major haplotypes of all populations were SH1 and SH2 implying they might be the ancestral haplotypes. The topological structures of the Bayesian inference and maximum likelihood trees were similar. They were composed of two major haplotype branches with a high posteriori probability or support rate and several hybrid haplotype branches (Figs. 4 and 5).

The molecular variance analysis in Table 2 shows that only 7.29% of the variation was observed between populations, while 92.71% was observed within populations. The variation among lineages (56.90%) was greater than that among the individuals within a lineage (43.1%), and the value of Φ_{ST} was high and significant. A significant genetic differentiation was observed among the lineages, which might have an independent demographic history.

The population genetic structure analysis results (Tab. 3) showed that the mean and standard deviation of the nucleotide difference was 11.0309 ± 1.2332. The mean value of the nucleotide difference in LK was the largest (11.0309 ± 1.2332), while that in the WH population was the smallest (9.5037). The Φ_{ST} and net nucleotide between the LK and WH populations was the largest, which were 0.1947 and 2.9070, respectively. The average Φ_{ST} and net nucleotide between LK and other wild populations were 0.1592 ± 0.0255 and 2.3730 ± 0.4426, respectively, which were larger than those of the largest values among wild populations (0.0602 and 0.6248).

3.3 Demographic history and divergence time

Although the most sensitive R^2 test did not result in any significant value. On the contrary, the D value of the Tajima test (1.3302, −1.2243) and Fu's Fs test value (−12.6557, −12.1367) of lineages 1 and 2 were negative, and Fu's Fs test values of the two lineages were significant (0.0010, 0.0010). The neutral evolution hypothesis was rejected, and lineages 1 and 2 might experience population expansion events. However, lineage 3 could not completely reject the neutral evolution hypothesis (Tab. 4).

The nucleotide mismatch distribution of lineages 1 and 2 showed a unimodal shape (Fig. 6). According to the divergence rate of 3–10% per million years in the mtDNA control region, the expansion times of lineages 1 and 2 were estimated at 332.5–99.8 and 393.2–113.0 thousand years ago, respectively.

The Bayesian skyline analysis showed that all lineages experienced an increase in effective population size (Fig. 7). According to the divergence rate of 3–10% per million years in the control region, the fastest growth rates of lineages 1 and 2 were 60–200 and 45–150 million years ago, respectively.

The pairwise differences values between XM population and other populations were positive except for HA population (−0.0845) (Tab. 3), indicating genetic divergence between XM population and other Chinese populations. Genetic exchange was existed among ZS, WH and RZ populations for the values of pairwise differences among them were negative. Significant differences were revealed between LK and HA, LK and XM, while extremely significant differences were discovered between LK and the remaining populations. The cultured population (LK) displayed greater genetic variation, which might be related with the higher level of nucleotide diversity (π).

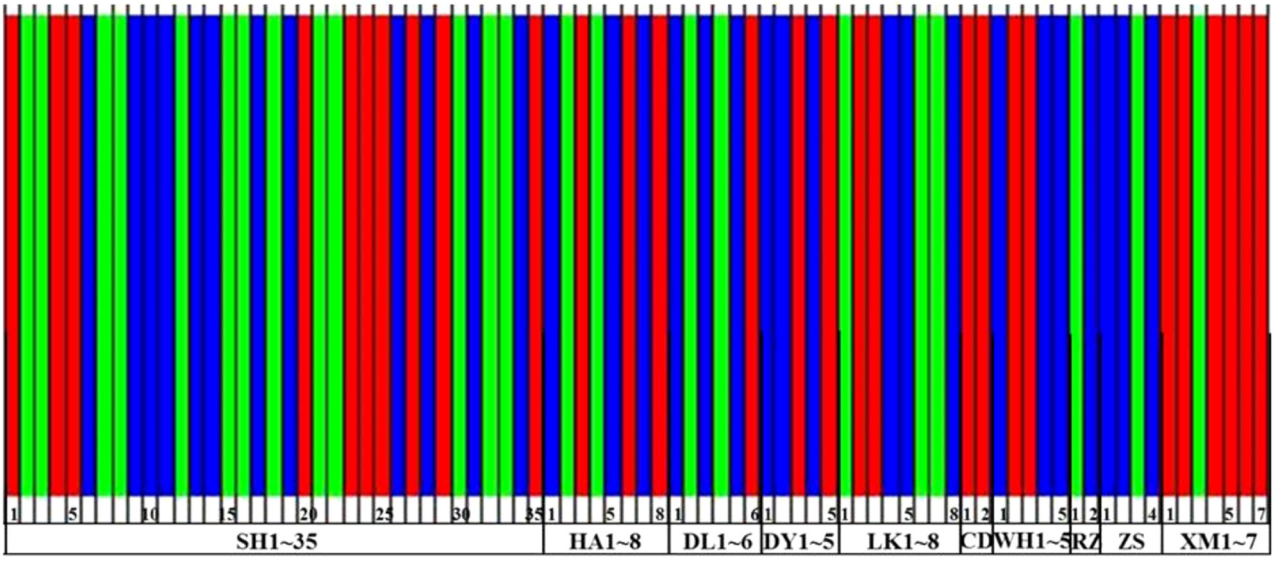

Fig. 2. Bayesian clustering analysis of *T. modestus* haplotypes.

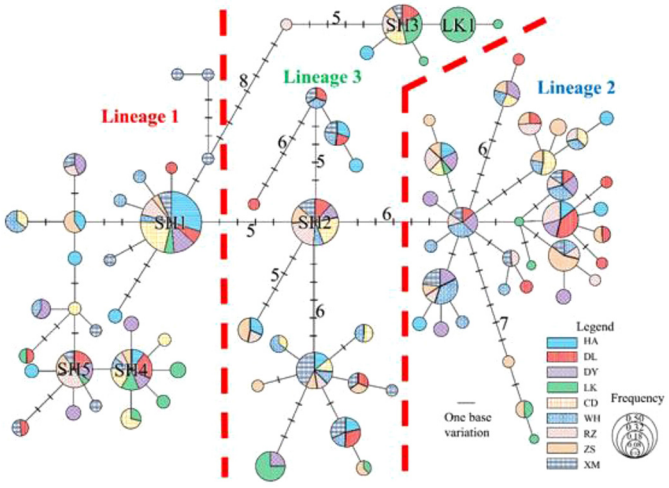

Fig. 3. Haplotype median-joining network of *T. modestus*.

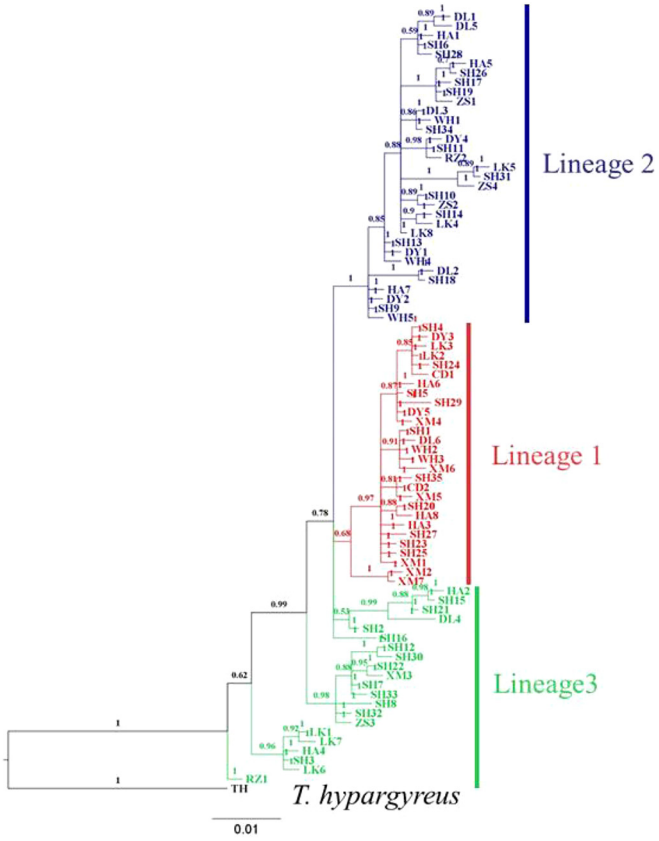

Fig. 4. Bayesian inference (BI) tree of haplotypes in *T. modestus*.

4 Discussion

4.1 Species identification and taxonomic

The distribution of "green fin" filefish is mainly related to the offshore waters of China, Japan and South Korea in Northwest Pacific Ocean. Most of the related studies in these countries used *T. modestus* as its scientific name (Kwon et al., 2007; Mizuno et al., 2012; An et al., 2013), and Japanese taxonomic books suggested that *T. modestus* should be the unified scientific name (Yamada et al., 2007). In addition, the sequences obtained in our study were consistent with the complete mitochondrial genome of *T. modestus* (GenBank accession number: AP009185) on NCBI (Yamanoue et al., 2008). Therefore, we used *T. modestus* as the scientific name in our study.

According to the sequence of the hypervariable mtDNA control region of *T. modestus*, although some hierarchical structures were detected, the genetic differences were much smaller than those of *T. hypargyreus* (Li et al., 2016;

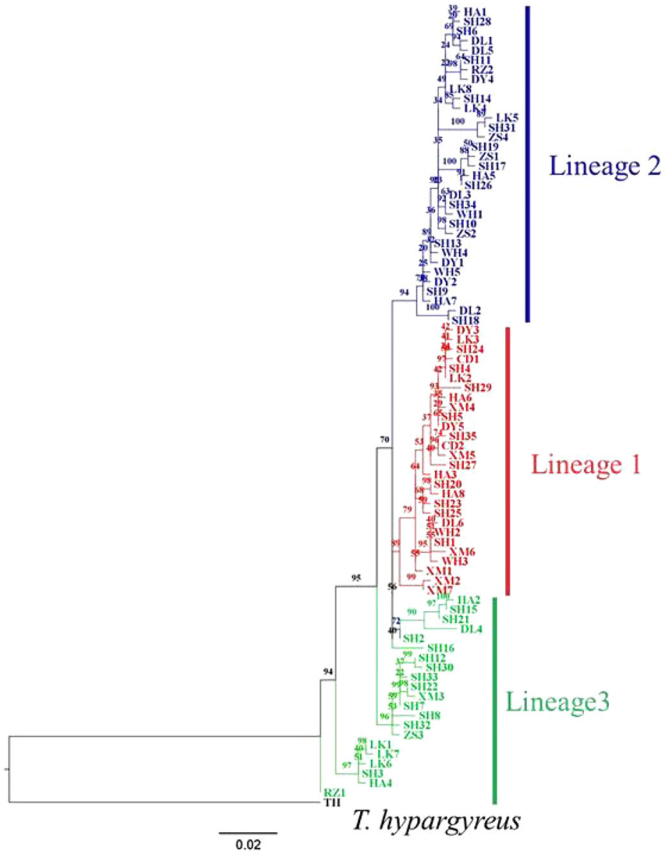

Fig. 5. Maximum likelihood (ML) tree of haplotypes in *T. modestus*.

Wang et al., 2016), and no significant correlation was observed between the hierarchical structure and the morphological characteristics (Wang, 2017). Meanwhile, the phylogenetic studies based on mitochondrial COI, Cyt *b* and the complete sequence of the control region also showed only three species (*T. modestus*, *T. hypargyreus* and *T. tessellatus*) in genus *Thamnaconus* in the samples collected from the locations (Wang, 2017). The intraspecific genetic differences of *T. modestus* were obviously smaller than its genetic differences among the three species. The phylogenetic analysis also verified that the collected samples were of the species.

4.2 Comparison of population genetic diversity and genetic structure

The number of effective parents in farmed populations is commonly smaller than that in wild populations. Low numbers of effective parents results in small genetic offspring diversity, leading to inbreeding depression, highlighting the importance of the selection of parents (Charlesworth, 2003). Meanwhile, the cultivation method for maximising economic benefits may exert an artificial selection pressure on the offspring, resulting in the decrease of the genetic diversity of the breeding population. In this study, the haplotype diversity of the LK cultured population was significantly lower than those of other wild populations; only18 haplotypes were identified in the 50 fish samples, which might be mainly caused by the limited

Table 2. Analysis of molecular variation in *T. modestus*.

Source of variation	Variance components	Percentage of variation	Φ Statistics	*P*
Among lineages	4.22	56.90	$\Phi_{ST} = 0.57$	0.0000
Within lineages	3.22	43.10		
Among populations	0.44	7.29	$\Phi_{ST} = 0.07$	0.0000
Within populations	5.64	92.71		

number of effective parents and the high contribution rate of certain parents in the cultured population. Meanwhile, the nucleotide diversity of the LK cultured population was the highest, and the genetic differences among the haplotypes were large, which might be related to the large genetic differences among the parents and the great artificial selection pressure. Significant genetic differences were observed between the LK cultured and wild populations, and the breeding process was speculated to have changed the population genetic structure (An et al., 2011; Yi et al., 2015). Avoiding the escape of offspring, paying close attention to the health status of the aquaculture population and carefully using the population for resource recovery are imperative.

The haplotype and nucleotide diversities of the wild population were high, the population had three lineages and the genetic divergence within the population was high. The wide range of activities, clustering, short sexual maturation cycle and large spawning capacity of *T. modestus* determine its r-selection biological history (Pu and Xu, 1985; Zheng et al., 1990). Long-distance migration, the long planktonic stage of fish roe and larvae and the Northwest Pacific circulation enhanced the gene connectivity and formed a mixed genetic structure within the population. Although the *T. modestus* distributed in different seas owned different external morphological traits and living habits, they might only be affected by environmental factors (mainly water temperature). Hence, no significant population genetic structure was formed. However, on the aspects of fisheries resources management, restoration and sustainable utilisation, especially in relation to proliferation and release, strict hierarchical analysis must be performed for the genetic structure and genetic diversity of released individuals to be generally consistent with the local population.

Genetic divergences were examined between XM population and other Chinese populations, perhaps it was because of the far distances from other locations and weak gene flow. However, the lower pairwise difference values of ZS, WH and RZ populations meant frequent genetic communication due to the Yellow Sea Warm Current and Coast Current, no obvious geographical barriers existing among them. While, other populations (CD, DL, DY, LK) were located inside the Bohai Bay, and the Shandong peninsula might block gene flow between them.

4.3 Genetic lineage structure and demographic history

Historical allopatric distribution, niche differentiation and so on are the causes of lineage structure (Pelletier et al., 2015; Hu et al., 2015). A significant hierarchical structure was

Table 3. Corrected average pairwise differences (above diagonal) and Φ_{ST} values (below diagonal) between populations and average number of pairwise differences on the diagonal within population.

	HA	DL	DY	LK	CD	WH	RZ	ZS	XM
HA	10.8572	−0.1373	−0.0676	2.2131*	−0.1770	0.1950	0.1614	0.4529	−0.0845
DL	−0.0128	12.3917	−0.1963	2.2964**	0.1322	−0.0816	−0.1732	0.0547	0.1345
DY	−0.0069	−0.0200	9.8406	2.7917**	0.1122	−0.0349	−0.0538	0.0777	0.3302
LK	0.1490*	0.1513**	0.1824**	13.1597	1.8222**	2.9070**	2.3263**	2.8460**	1.7814*
CD	−0.0168	0.0106	0.0106	0.1277**	10.4214	0.6248	0.4345	0.7317	0.0656
WH	0.0195	−0.0082	−0.0034	0.1947**	0.0592	9.5037	−0.1539	−0.1298	0.3794
RZ	0.0152	−0.0154	−0.0060	0.1600**	0.0398	−0.0159	10.5165	−0.2048	0.3927
ZS	0.0371	0.0044	0.0049	0.1820**	0.0602	−0.0126	−0.0184	12.0774	0.5722
XM	−0.0078	0.0114	0.0306	0.1265*	0.0062	0.0363	0.0360	0.0482	10.5095

One asterisk means significant difference ($0.01 \leq P < 0.05$), and two asterisks mean extremely significant difference ($P < 0.01$).

Table 4. Parameters of mismatch distribution analysis.

	Harpending raggedness index	Demographic expansion model			Spatial expansion model		
		Tau	SSD	*P*	Tau	SSD	*P*
Lineage 1	0.0313	4.64	0.1497	0.0900	4.22	0.0101	0.6300
Lineage 2	0.0132	4.99	0.0022	0.3300	4.78	0.0016	0.8000

detected in *T. modestus* but no obvious correlation was observed between the hierarchical structure and the geographic distribution. According to the results of demographic history analysis, population expansion occurred at the end of Pleistocene, and each lineage was speculated to be formed by different shelters during the Pleistocene glacial period. Lineages 1 and 2 were the main refuge lineages, while lineage 3 was a collection of small adjacent shelters. The low ocean temperature and sea level in the Pleistocene glacial period resulted in the shrinkage of habitat and the disappearance of some creatures, especially in the last glacial maximum, with the sea level falling by 130 m (Hewitt, 2000; Clark et al., 2009). *T. modestus* was a warm-temperature fish, and the vast continental shelf of Northwest Pacific and the influx of the Kuroshio Current provided it with a vast and suitable habitat. During the last glacial peak of Pleistocene, polar glaciers prevailed, and the continental shelf was exposed to the sea. In addition, the sea water temperature dropped significantly along with the evident weakening of Kuroshio Current. East China Sea Trough, the eastern coast of Taiwan and Central South China Sea were presumed the only residual shelters suitable for *T. modestus*. Geographical isolation resulted in significant genetic differences among the populations under the effect of random genetic drift, which left a deep impression within the hierarchical structure and formed the three lineages today. However, the sea level rose after the last ice peak and the geographic isolation was broken, causing heterogenous populations from different lineages to mix again. However, the lineage structure still did not disintegrate rapidly with the increase of the gene flow among the populations. The long-term ice isolation effect that caused significant genetic differences among the lineages was greater than that of the

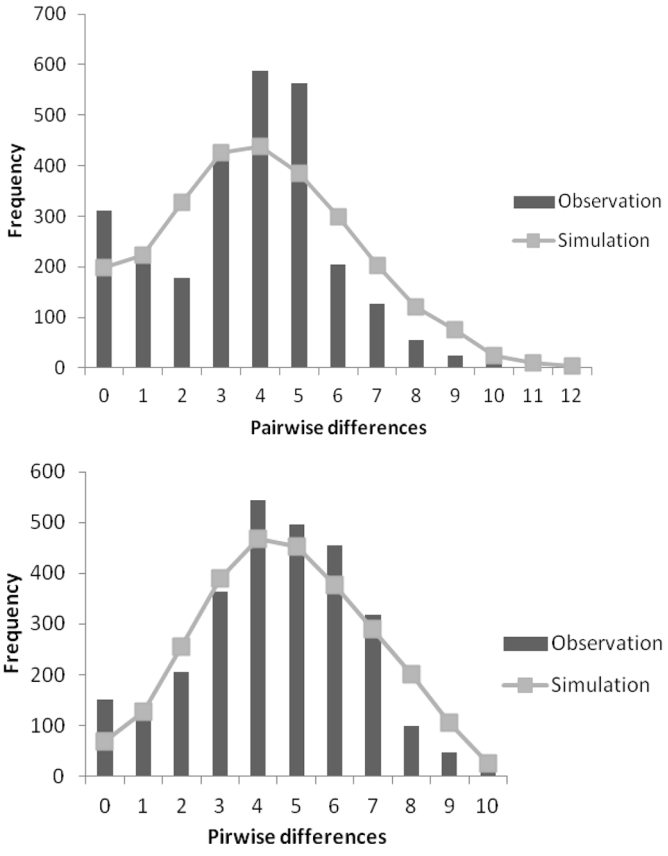

Fig. 6. Mismatch distribution analysis of lineage 1 and lineage 2 (from top to bottom).

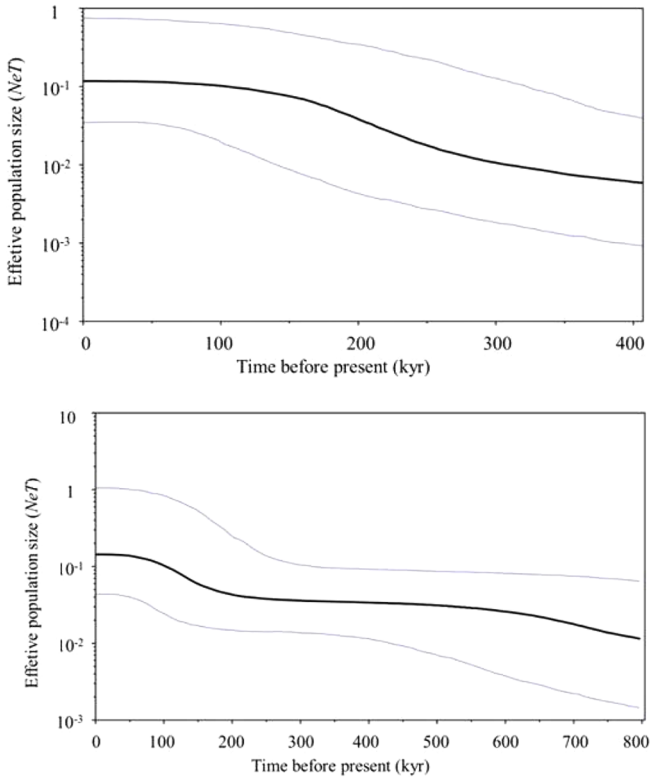

Fig. 7. Bayesian skyline analysis of lineage land lineage 2 (from top to bottom).

post-ice gene exchange. Given the wide range of activities, no significant correlation existed between the lineages of *T. modestus* and the geographical distribution. The special geological structure and current characteristics of Northwest Pacific Ocean together with the life history of *T. modestus* contributed to the phylogenetic structure, which was highly differentiated and spatially distributed in the same region. The species with the same phylogenetic structures in the adjacent sea areas, such as *Lateolabrax japonicus* (Liu et al., 2006) and *Scomber japonicus* (Yan et al., 2015), were also detected.

As an important marine commercial fish, the fishing intensity of *T. modestus* in different sea areas must be allocated according to the population structure during fisheries management. Traditional genetic research techniques use limited gene loci for analysis, which could not meet the need for an accurate assessment of population genetic differentiation. With the development of the next-generation sequencing (NGS) technology, it is expected to reveal the genetic diversity of *T. modestus* based on the entire genome in future study.

Acknowledgements. We thank Prof Dianrong Sun, Prof Longshan Lin, Mr Jianwei Zou, Ms Pengfei Li, Mr Binbin Shan and Dr Yuan Li for assistance in collecting samples. We are also grateful to Mr Wei Zhou for technical assistance and Dr Wei Meng for proofreading the manuscript. This work was supported by Fund of Key Laboratory of South China Sea Fishery Resources Exploitation & Utilization, Ministry of Agriculture, P. R. China (FREU2017-05); the National Natural Science Foundation of China (41776171); and the Scientific Research Startup Foundation of Zhejiang Ocean University (2016-2017).

References

An HS, Kim EM, Lee JH, Noh Jk, An CM, Yoon SJ, Park KD, Myeong JI. 2011. Population genetic structure of wild and hatchery black rockfish Sebastes inermis in Korea, assessed using cross-species microsatellite markers. *Genet Mol Res* 10: 2492–2504.

An HS, Lee JW, Park JY, Jung HT. 2013. Genetic structure of the Korean black scraper *Thamnaconus modestus* inferred from microsatellite marker analysis. *Mol Biol Rep* 40: 3445–3456.

Bouckaert R, Heled J, Kühnert D, Vaughan T, Wu CH, Xie D, Suchard MA, Rambaut A, Drummond AJ. 2014. BEAST 2: a software platform for bayesian evolutionary analysis. *Plos Comput Biol* 10: e1003537.

Charlesworth D. 2003. Effects of inbreeding on the genetic diversity of populations. *Philos T R Soc B* 358: 1051–1070.

Chen WZ, Li CS, Hu F. 2000. Application and improvement of virtual population analysis (VPA) in stock assessment of *Thamnaconus septentrionalis*. *J Fish Chin* 24: 522–526.

Clark PU, Dyke AS, Shakun JD, Carlson AE, Clark J, Wohlfarth B, Mitrovica JX, Hostetler SW, McCabe AM. 2009. The Last Glacial Maximum. *Science* 325: 710–714.

Corander J, Waldmann P, Marttinen P, Sillanpää MJ. 2004. BAPS 2: enhanced possibilities for the analysis of genetic population structure. *Bioinformatics* 20: 2363–2369.

Drummond AJ, Bouckaert RR. 2015. Bayesian and evolutionary analysis with BEAST. Cambridge: Cambridge University Press.

Darriba D, Taboada GL, Doallo R, Posada D. 2012. jModelTest 2: more models, new heuristics and parallel computing. *Nature methods* 9: 772.

Domingues RR, Hilsdorf AWS, Shivji MM, Hazin FVH, Gadig OBF. 2018. Effects of Pleistocene on the mitochondrial population genetic structure and demographic history of the silky shark (*Carcharhinus falciformis*) in the western Atlantic Ocean. *Rev Fish Biol Fisher* 28: 213–227.

Donaldson KA, Wilson RR. 1999. Amphi-panamic geminates of snook (Percoidei: Centropomidae) provide a calibration of the divergence rate in the mitochondrial DNA control region of fishes. *Mol Phylogenet Evol* 13: 208–213.

Excoffier L, Lischer HEL. 2010. ARLEQUIN suite ver 3.5: a new series of programs to perform population genetics analyses under Linux and Windows. *Mol Ecol Resour* 10: 564–567.

Fu YX. 1997. Statistical tests of neutrality of mutations against population growth, hitchhiking and background selection. *Genetics* 147: 915–925.

Hatab S, Chen ML, Miao WH, Lin JH, Wu DD, Wang CY, Yuan PX, Deng SG. 2017. Protease Hydrolysates of Filefish (*Thamnaconus modestus*) Byproducts Effectively Inhibit Foodborne Pathogens. *Foodborne Pathog Dis* 7: 325–335.

Hewitt GM. 2000. The genetic legacy of the Quaternary ice ages. *Nature* 405: 907–913.

Hu JH, Jiang ZG, Chen J, Qiao HJ. 2015. Niche divergence accelerates evolution in Asian endemic *Procapra* gazelles. *Sci Rep* 5: 10069.

Iguchi K, Tanimura Y, Nishida M. 1997. Sequence divergence in the mtDNA control region of amphidromous and landlocked forms of ayu. *Fisheries Sci* 63: 901–905.

Kim AR, Bae HJ, Kim HG, Oh CW. 2016. Age and growth of filefish, *Thamnaconus modestus* (Günther, 1877) off the Jeju Island of Korea. *Ocean Sci J* 51: 355–362.

Kwon JH, Kausar T, Noh J, Kim DH, Byun MW, Kim KS, Kim KS. 2007. The identification of irradiated seasoned filefish (*Thamnaconus modestus*) by different analytical methods. *Radiat Phys Chem* 76: 1833–1836.

Li PL, Jiang MC, Xu JB, Liu B. 2002. Marine cage-culture technology of *Thamnaconus modestus*. *China Fish* 8: 61–62.

Li YF, Chen GB, Yu J, Wu SQ, Xiong D, Li X, Cui K, Li YZ. 2016. Population genetics of *Thamnaconus hypargyreus* (Tetraodontiformes: Monacanthidae) in the South China Sea. *Mitochondrial DNA A*, 27: 798–805.

Liu JX, Gao TX, Yokogawa K, Zhang YP. 2006. Differential population structuring and demographic history of two closely related fish species, Japanese sea bass (*Lateolabrax japonicus*) and spotted sea bass (*Lateolabrax maculatus*) in Northwestern Pacific. *Mol Phylogenet Evol* 39: 799–811.

Liu K, Zhang LL, Zhang QW, Chen SQ, Liu CL, Bian L. 2017. Study on *Thamnaconus septentrionalis* under industrial aquaculture condition. *Fishey Modernization* 44: 35–40.

Liu M, Lu ZC, Gao TX, Yanagimoto T, Sakurai Y. 2010. Remarkably low mtDNA control region diversity and shallow population structure in Pacific cod *Gadus macrocephalus*. *J Fish Biol* 77: 1071–1082.

Miyajima-Taga Y, Masuda R, Yamashita Y. 2017. Feeding capability of black scraper *Thamnaconus modestus* on giant jellyfish *Nemopilema nomurai* evaluated through field observations and tank experiments. *Environ Biol Fish* 100: 1237–1249.

Mizuno K, Shimizu-Yamaguchi S, Miura C, Miura T. 2012. Method for efficiently obtaining fertilized eggs from the black scraper *Thamnaconus modestus* by natural spawning in captivity. *Fisheries Sci* 78: 1059–1064.

NFRDI. 2009. Research on actual fisheries state and biological characteristic of *Thamnaconus modestus*, 2009. National Fisheries Research and Development Istitute, Busan, NFRDI Research Paper.

Nguyen LT, Schmidt HA, von Haeseler A, Minh BQ. 2015. IQ-Tree: a fast and effective stochastic algorithm for estimating maximum-likelihood phylogenies. *Mol Biol Evol* 32: 268–274.

Pelletier TA, Crisafulli C, Wagner S, Zellmer AJ, Carstens BC. 2015. Historical Species Distribution Models Predict Species Limits in Western Plethodon Salamanders. *Syst Biol* 64: 909–925.

Pu ZS, Xu YM. 1985. Analysis of *Navodon septentrionalos* populations in the east China sea. *Marin Fish* 7: 6–11.

Qian SX, Hu YZ. 1980. A Preliminary study on the age and growth of filefish (*Navodon septentrionalos*). *J Fisheries China* 4: 197–206.

Ramos-Onsins SE, Rozas J. 2002. Statistical properties of new neutrality tests against population growth. *Mol Biol and Evol* 19: 2092–2100.

Rice WR. 1989. Analyzing tables of statistical tests. *Evolution* 43: 223–225.

Ronquist F, Teslenko M, van der Mark P, Ayres DL, Darling A, Höhna S, Larget B, Liu L, Suchard MA, Huelsenbeck JP. 2012. MrBayes 3.2: efficient bayesian phylogenetic inference and model choice across a large model space. *Systematic Biol* 61: 539–542.

Rozas J, Ferrer-Mata A, Sánchez-DelBarrio JC, Guirao-Rico S, Librado P, Ramos-Onsins SE, Sánchez-Gracia A. 2017. DnaSP 6: DNA Sequence Polymorphism Analysis of Large Data Sets. *Mol Biol Evol* 34: 3299–3302.

Sambrook J, Russell DW. 2001. *Molecular Cloning: A Laboratory Manual*, third ed. New York: Cold Spring Harbor Laboratory Press.

Song N, Ma GQ, Zhang XM, Gao TX, Sun DR. 2013. Genetic structure and historical demography of *Collichthys lucidus* inferred from mtDNA sequence analysis. *Environ Biol Fish* 97: 69–77.

Stewart DT, Baker AJ. 1994. Patterns of sequence variation in the mitochondrial D-loop region of shrews. *Mol Biol Evol* 11: 9–21.

Su JX, Li CS. 2002. *Fauna Sinica Osteichthyes Tetraodontiformes Pegasiformes Gobiesociformes Lophiiformes*. Beijing: Science Press.

Tajima F. 1989. Statistical method for testing the neutral mutation hypothesis by DNA polymorphism. *Genetics* 123: 585–595.

Wang SM. 1988. A preliminary study on *Thamnaconus modestus* in the Yellow Sea and Bohai Sea. *Marin Fish* 1: 16–19.

Wang ZY, Zhang Y, Zhao LL, Song N, Han ZQ, Gao TX. 2016. Shallow mitochondrial phylogeographical pattern and high levels of genetic connectivity of *Thamnaconus hypargyreus* in the South China Sea and the East China Sea. *Biochem Syst Ecol* 67: 110–118.

Wang ZY. 2017. *Molecular phylogeography and phylogenetic analysis of Thamnaconus and Platycephalus in China seas*. Qingdao: Ocean University of China.

Yamada U, Tokimura U, Horikawa H, Nakabo T. 2007. *Fishes and fisheries of the East China and Yellow Seas*. Kanagawa: Tokai University Press.

Yamanoue Y, Miya M, Matsuura K, Katoh M, Sakai H, Nishida M. 2008. A new perspective on phylogeny and evolution of tetraodontiform fishes (Pisces: Acanthopterygii) based on whole mitochondrial genome sequences: Basal ecological diversification? *BMC Evol Biol* 8: 212–220.

Yan S, Catanese G, Brown CL, Wang M, Yang CP, Yang TB. 2015. Phylogeographic study on the chub mackerel (*Scomber japonicus*) in the Northwestern Pacific indicates the late Pleistocene population isolation. *Mar Ecol-Evol Persp* 36: 753–765.

Yi TL, Guo WJ, Liang XF, Yang M, Lv LY, Tian CX, Song Y, Zhao C, Sun J. 2015. Microsatellite analysis of genetic diversity and genetic structure in five consecutive breeding generations of mandarin fish *Siniperca chuatsi* (Basilewsky). *Genet Mol Res* 14: 2600–2607.

Zheng YJ, Fang RS, Yao WZ, Zhou RK, Lu WM. 1990. Studies on populations of greenfin filefish in the East Yellow Sea and the southwest Japan Sea. *Mar Fish* 12: 202–208.

Cite this article as: Yang T, Wang Z, Liu Y, Gao T. 2019. Population genetics and molecular phylogeography of *Thamnaconus modestus* (Tetraodontiformes, Monachanthidae) in Northwestern Pacific inferred from variation of the mtDNA control region. *Aquat. Living Resour.* 32: 18